Original Article

Vol. 9, No. 1; 2025; pp 12–18
DOI: https://doi.org/10.26676/jevtm.49156

Establishing a Swine Model of Acute Respiratory Distress Syndrome Secondary to Ischemia-Reperfusion Injury Following Acute Limb Ischemia

Grzegorz Jodlowski[1], Rebecca Treffalls[1], May Dvir[1], Silvana N Wilken[2], Jonathan J Morrison[1] and Patrick F Walker[3]

[1]Department of Endovascular and Vascular Surgery, Mayo Clinic, Rochester, Minnesota, USA
[2]Department of Surgery, Mayo Clinic, Rochester, Minnesota, USA
[3]Department of Surgery, Uniformed Services University of the Health Sciences, Bethesda, Maryland, USA

Background: Acute Respiratory Distress Syndrome (ARDS) is a severe complication of ischemia-reperfusion injury (IRI), characterized by acute hypoxemic respiratory failure and high mortality. Acute limb ischemia (ALI) can trigger systemic inflammation leading to ARDS. This study introduces a swine model of ARDS secondary to ALI.
Methods: Two Yorkshire swine were used in this study. Animals were anesthetized and subjected to nine hours of hindlimb ischemia via arterial occlusion. The limb was then reperfused and animals monitored through physiological parameters, computed tomography imaging, lung ultrasounds and histology. Data was then analyzed using GraphPad Prism and Analyze software for statistical and imaging evaluation.
Results: Baseline measurements confirmed normal vasculature and stability, access was obtained and occlusion delivered. Following nine hours of hindlimb ischemia, reperfusion led to progressive respiratory decline, with worsening oxygenation, decline in the Horowitz index, elevated lactate and potassium levels, and imaging showing early signs of lung injury. Post-mortem analysis confirmed lung congestion, consistent with ARDS.
Conclusions: The study demonstrates a novel, easily performed, cost-effective and replicable swine model of ARDS using hindlimb IRI. This model mimics physiological and sterile conditions seen in a clinical setting and serves as a valuable tool for studying ARDS. It also allows for investigation of the systemic inflammatory cascade triggered by peripheral ischemia, mirroring human ARDS cases that occur with distal injuries. Future studies with larger sample sizes and extended critical care periods are recommended to validate the technique and enhance its relevance for experimental applications.

Keywords: *ARDS; ALI; Swine Model; Ischemia Reperfusion Injury*

Received: 27 March 2025; Accepted: 10 April 2025

INTRODUCTION

Acute Respiratory distress syndrome (ARDS) is recognized as one of the most severe manifestations of organ dysfunction following ischemia-reperfusion injury (IRI) [1]. ARDS is defined as acute hypoxemic respiratory failure with bilateral pulmonary infiltrates on chest X-ray or computed tomography (CT) of a non-cardiac origin, and a Horowitz index (PaO_2/FiO_2; the ratio of partial pressure of oxygen in arterial blood to the fraction of inspiratory oxygen concentration) for lung function of less than 300 mmHg. The incidence of ARDS in the United States is estimated to be between 62.2 and 78.9 cases per 100,000, among which 75% is moderate or severe. The overall mortality was evaluated at 43% [2,3]. Although intensively investigated for years, the fundamental mechanisms contributing to ARDS have not been completely understood [3].

Acute limb ischemia (ALI) is defined as a sudden decrease in limb arterial perfusion that jeopardizes limb viability [4]. It is a common vascular emergency, with an incidence of 22–26 per 100,000 patients per year [5].

Corresponding author:
Jonathan J. Morrison, Senior Associate Consultant, Division of Vascular and Endovascular Surgery, 507-284-4494, Mayo Clinic, 200 First Street SW, Rochester, MN 55905, USA.
Email: morrison.jonathan@mayo.edu

One of the consequences of revascularization is IRI, defined as worsening of cellular dysfunction and death following restoration of the blood flow to previously ischemic tissues. The mechanism behind the phenomenon is mostly related to dysregulation of metabolic pathways during ischemia, accumulation of metabolites and generation of reactive oxygen species (ROS) with reintroduction of oxygen during reperfusion [6]. This is particularly important in large-scale combat operations, such as the war in Ukraine, where, due to loss of air supremacy, the tourniquet time is significantly prolonged [7]. More notably though, this process is not limited to the affected area (for instance, the limb), but may lead to extensive systemic insult with multiple organs, including ARDS [8]. Alongside its high mortality, ARDS is very costly to manage, as these patients require prolonged intensive care hospitalization, and there are limited therapeutic modalities available to combat this condition.

This has necessitated the creation of a reliable, reproducible and cost-effective animal model for further investigations and translational research to develop new therapies for ARDS. Commonly described animal models of ARDS were established by surfactant washout, oleic acid (OA) intravenous injection or lipopolysaccharide (LPS) injection. These, however, differ from the actual pathomechanism of lung insult [9]. A physiologically comparable model was implemented by inducing pulmonary ischemia by clamping the pulmonary artery, the bronchial artery, and the bronchus in the affected lung, but this model requires a rather complex and invasive surgical approach [1].

In the current work we propose a swine model of ARDS secondary to ALI. In this setting, in a time-dependent manner, the corresponding reperfusion injury releases a systemic burst of pro-inflammatory mediators and ROS, precipitating non-cardiogenic pulmonary edema. This approach offers a practical, physiological, less invasive and more accessible alternative to traditional ARDS models, which are often complex and costly. Facilitating this model in the medical field could enhance the understanding of ARDS mechanisms and allow preclinical studies of novel therapies with better translatability.

METHODS

Study Design and Overview

Before commencing the experimental protocol, approval from the Institutional Animal Care and Use committee was achieved. The animal facility is accredited by the American Association of Laboratory Animal Sciences.

Two female Yorkshire swine weighing between 47 kg and 52 kg were enrolled in the study. ARDS was induced using a three-phase process: animal preparation, hindlimb ischemia and reperfusion induced ARDS.

Animal Preparation

The animals were initially sedated with telazol (5 mg/kg) and xylazine (2 mg/kg) via intramuscular injection. The animals were transported to the laboratory where they were endotracheally intubated and general anesthesia was maintained using intravenous propofol. The animals were mechanically ventilated using a volume-controlled mode with a tidal volume of 8–12 ml/kg, FiO_2 60%, positive end-expiratory pressure (PEEP) at 5 cmH_2O and a respiratory rate titrated to maintain an end-tidal CO_2 between 30 and 40 mmHg. This is standard for large animal studies in our laboratory.

Ultrasound-guided percutaneous vascular access was obtained in the left common carotid artery (5 Fr) using a modified Seldinger technique. Intravenous catheters were inserted into bilateral ear veins for propofol administration and maintenance fluids. Under fluoroscopic guidance, the left carotid artery was upsized to a 12 Fr DrySeal Flex Introducer sheath (Gore, Flagstaff AZ) over a 260 cm 0.035″ Glidewire Advantage (Terumo, Tokyo, Japan). A 5 Fr Pigtail catheter (AngioDynamics, Latham, NY) was inserted into the 12 Fr DrySeal sheath, and angiography was performed with a power injector to appreciate the anatomy of the terminal aortic trifurcation. The same pigtail catheter was then used for serial digital subtraction angiography.

Induction of Hindlimb Ischemia

To achieve hindlimb ischemia, two 260 cm 0.035″ Glidewire Advantage (Terumo, Tokyo, Japan) were inserted through the DrySeal sheath and advanced into the left external iliac artery (EIA) and middle sacral artery (MSA). A 6 Fr, 135 cm, 8 mm × 40 mm Mustang balloon (Boston Scientific, Marlborough, MA) and a 5 Fr, 135 cm, 6 mm × 20 mm Mustang balloon (Boston Scientific) were advanced into the EIA and MSA, respectively. An Endoflator (Boston Scientific) was used to inflate each balloon under fluoroscopy until each artery was occluded. A repeat angiogram was performed to confirm occlusion. Total endovascular occlusion of the left lower extremity was maintained for nine hours without any intervention.

Reperfusion-Induced ARDS

At the end of the nine hours, the left lower extremity was revascularized by restoring native inflow by deflating the common iliac artery balloon and the left MSA balloon. Animals were then observed with continuous physiological monitoring and serial arterial blood gas (ABG) analysis was performed.

Data Collection

During the experiment, PaO_2 and FiO_2 measurements were obtained from ventilator settings and ABGs. A post-reperfusion CT scan of the thorax was acquired six

hours after the beginning of reperfusion, alongside an ultrasound of the lungs. Histology samples of the lungs were collected following euthanasia.

Data Analysis

GraphPad Prism v8.0 (GraphPad Software Inc, San Diego, CA, USA) was used for visual representation of data and statistical analysis. CT scans were analyzed with the Analyze software (Analyze Direct, Overland Park, KS, USA). Histology samples were stained with hematoxylin and eosin (H&E) and reviewed under microscope (Zeiss, Axiovert 135 TV, Germany).

Ethical Approval

All animal procedures were approved by the Institutional Animal Care and Use Committee (IACUC) at Mayo Clinic (Protocol Number: A00007153-23) and were conducted in accordance with institutional and national guidelines for the care and use of laboratory animals.

RESULTS

Two female Yorkshire Swine were enrolled in the study. Instrumentation was successfully performed. Baseline angiogram was obtained depicting normal swine vasculature (Figure 1*a*). Baseline ABG measurements were obtained, with a lactate of 1.8–2.1 mmol/L and potassium of 4.2–4.5 mmol/L. Baseline FiO_2 was 59%, blood pressure 130/80 mmHg, heart rate 100 bpm, SpO_2 99%, respiratory rate 16 and end-tidal CO_2 30 mmHg. The baseline Horowitz index was calculated to be 503.9 and 510 mmHg, for each animal, respectively. Subsequently, EIA and MSA balloon occlusion was achieved, and confirmed with angiogram images (Figure 1*b*,*c*).

During the nine-hour occlusion phase, no significant events occurred, and the animals remained hemodynamically stable. Upon reperfusion, blood flow was restored (Figure 1*d*). The lactate was 1.9–2.0 mmol/L, the potassium 4.8–4.9 mmol/L and the Horowitz index 340–349.5 mmHg.

During the reperfusion-induced ARDS phase, oxygen saturation decreased to 92%, necessitating ventilator adjustments, including increasing FiO_2 to 100%, transitioning to pressure-controlled ventilation, raising PEEP while maintaining a plateau pressure below 30 cmH_2O, and implementing an inverse inspiration-to-expiration ratio greater than 1:1.

After six hours of reperfusion, lung imaging including ultrasound and CT was obtained depicting B-lines and dense consolidations, respectively (Figures 2 and 3). Lactate was recorded at 4.9–6.4 mmol/L and potassium was 5.3–6.1 mmol/L. The Horowitz index was at 110 mmHg, indicating moderately severe lung injury. The graph depicting Horowitz index changes is illustrated below (Figure 4).

At the end of the study, the lungs were inspected and post-mortem lung tissue were obtained. The tissue was stained with H&E, which revealed diffuse alveolar damage, inflammatory infiltrate and edema, consistent with early ARDS (Figure 5).

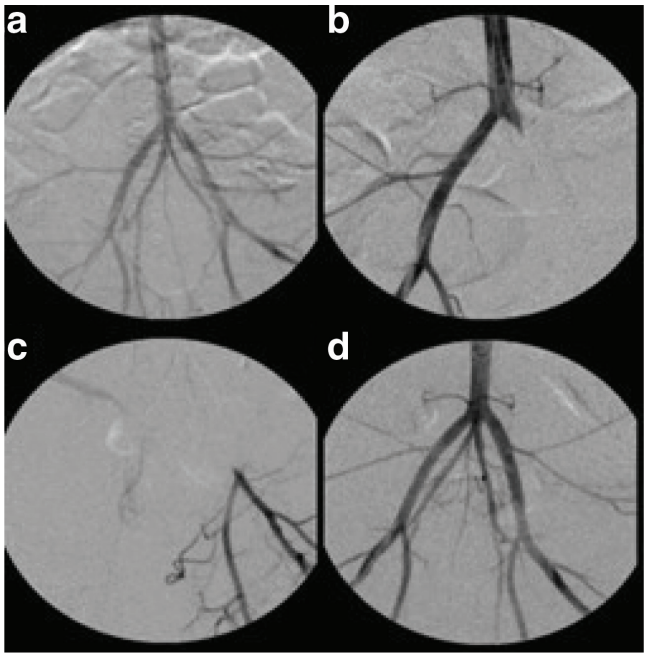

Figure 1 Representative digital subtraction angiography images: (**a**) baseline angiogram, (**b**) total balloon occlusion of the EIA and MSA, (**c**) tibial access confirmation and (**d**) post nine hours of occlusion.

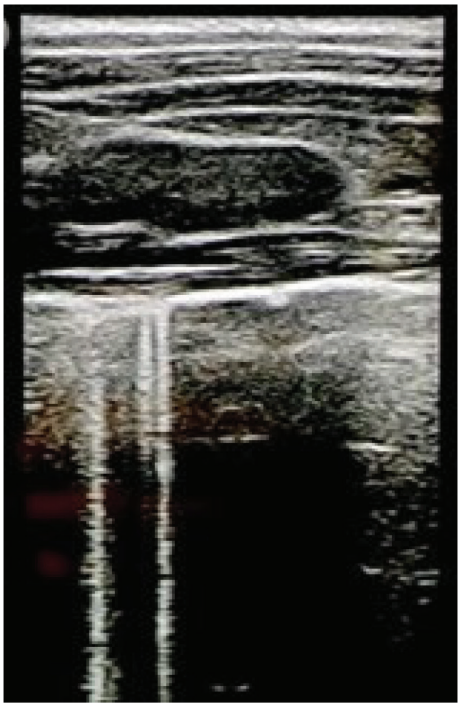

Figure 2 Lung ultrasound at the end of the study, depicting B-lines consistent with increased extravascular lung fluid.

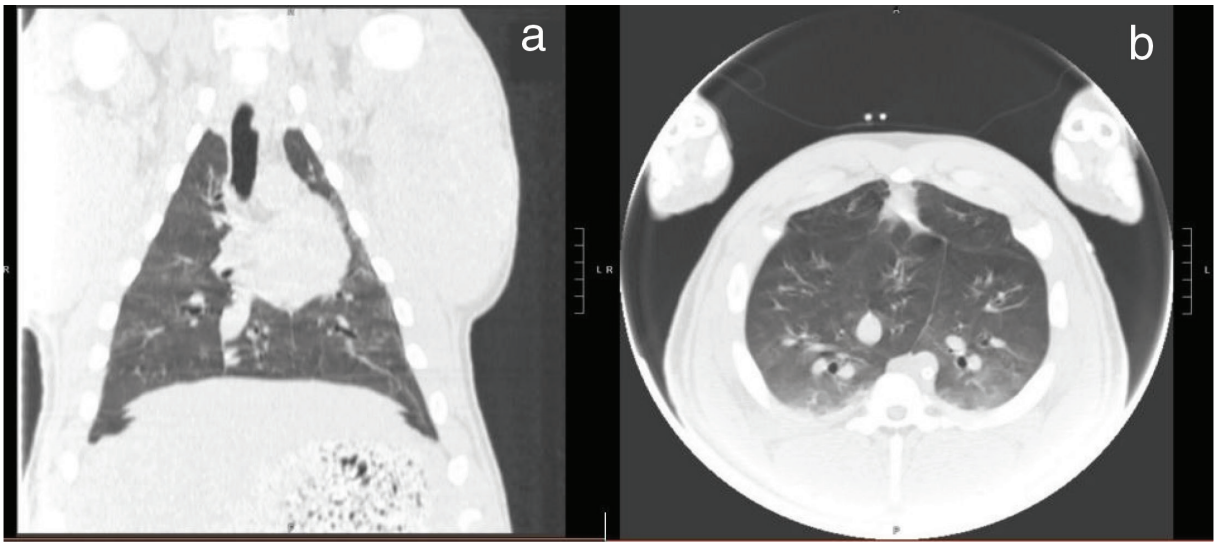

Figure 3 Chest computed tomography without contrast, axial plane (**a**) and coronal plane (**b**), at the end of the study, illustrating consolidation and ground-glass opacities, consistent with early ARDS.

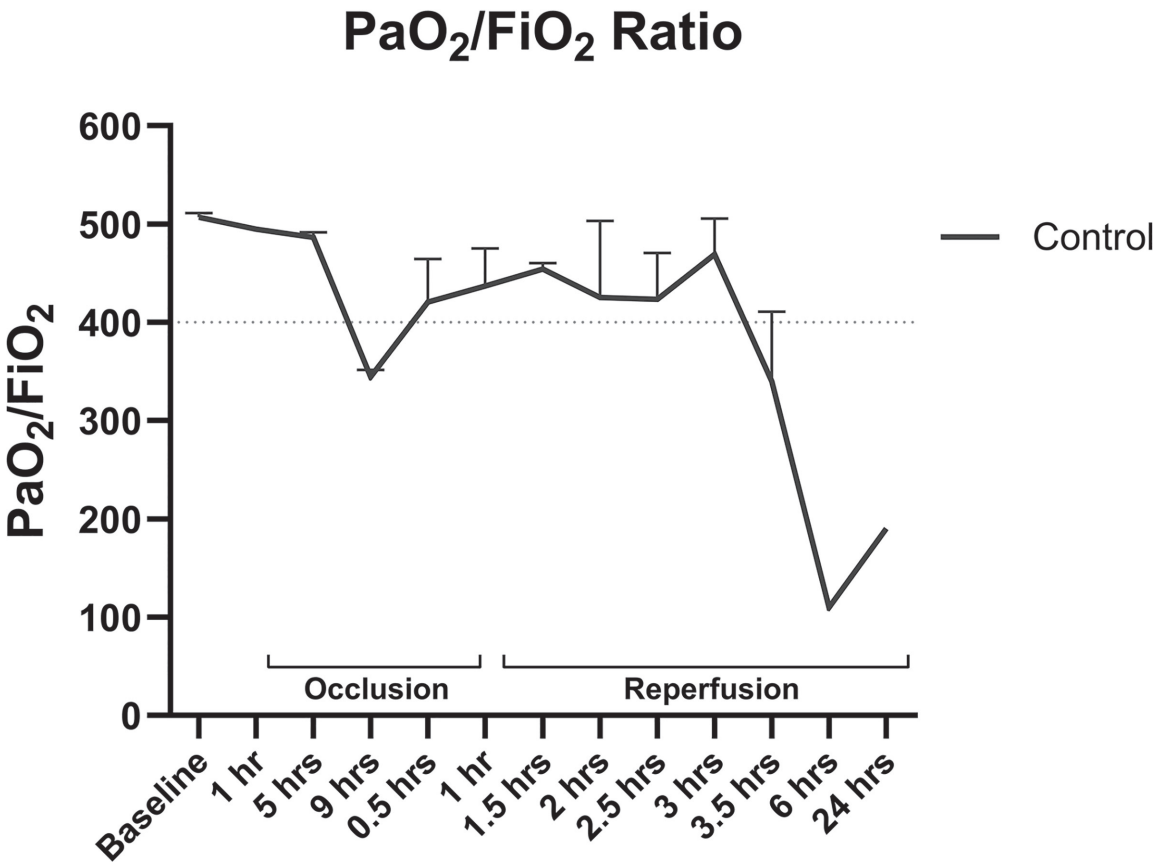

Figure 4 PaO_2/FiO_2 ratio in animals throughout the occlusion and reperfusion phases until euthanasia.

DISCUSSION

This study demonstrates a swine model of ARDS, implementing IRI by interrupting the blood supply to the hindlimb (Figure 6). This model has been shown to be easily performed, cost-effective and replicable. Furthermore, it serves as a valuable tool for studying ARDS, as it mimics physiological and sterile conditions, like those seen in a clinical setting. We have used a porcine model, as the anatomy, physiology, immune system and metabolism are more similar to humans compared to rodents, and the size allows for a broader spectrum of therapeutic testing [10].

Traditional animal ARDS models are important tools used by physicians and researchers to study the

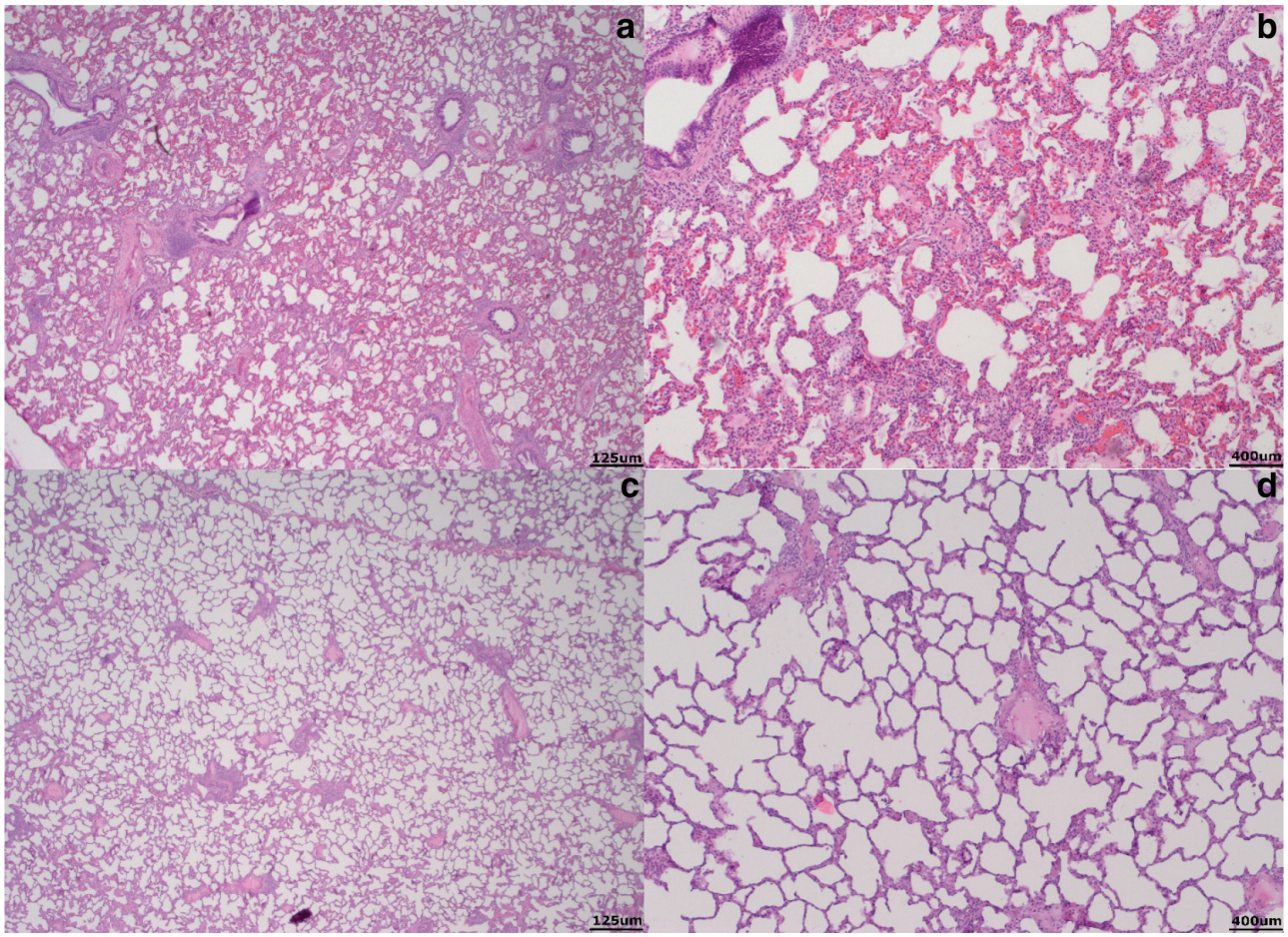

Figure 5 Histological sections of the lung stained with hemotoxylin and eosin ×12.5 magnification (**a**) and ×40 magnification (**b**) depicting pulmonary congestion and emphysema consistent with early ARDS, followed by ×12.5 magnification (**c**) and ×40 magnification (**d**) illustrating healthy lung tissue.

mechanisms and potential treatment options for this condition. While they provide valuable insights into the pathophysiological processes, none of them perfectly replicates all aspects of human ARDS [8]. The most used models are the lavage (LAV), OA and LPS models [6,9]. The LAV model, induced by repeatedly flushing the lungs with saline, primarily focuses on surfactant depletion and its consequences, including alveolar collapse [9]. This model is useful for studying the impact of different ventilation strategies and evaluating the potential therapies aimed at restoring surfactant friction. However, the LAV model does not inherently replicate the robust inflammatory response and permeability changes seen in ARDS [8,11]. In the OA model, OA is injected intravenously, leading to direct damage of the capillary endothelium and triggering the cascade of inflammatory response leading to ARDS. However, the main limitation lies in the distinct underlying cause, as ARDS very rarely results from fat embolism, the primary injury simulated in this model [8,12].

The third most popular model is created by injecting LPS, a component of bacterial cell walls and the aim is to replicate the pathophysiology of sepsis-induced ARDS, one of the most common ARDS etiologies [8,9]. LPS triggers a widespread inflammatory response, leading to lung injury, making this model valuable for exploring the inflammatory processes in ARDS and evaluating potential treatment targets. However, the LPS model often produces milder alveolar inflammation and permeability changes compared to those in ARDS. Additionally, the LPS model provides an incomplete representation of the effects of live bacteria, as it lacks direct cellular damage [8,9,13,14]. A slightly different approach was described where, instead of injecting LPS, mitochondrial damage-associated molecular patterns (DAMPs) were isolated and injected, replicating an inflammatory response comparable in severity to that seen in the LPS model [15]. It has also been shown that succinate, a marker of shock, global hypoxia and failure in energy production, can contribute to endotheliopathy in the gut, causing the release of LPS that further results in ARDS [16,17].

Pulmonary IRI models stimulate ARDS scenarios where lung injury arises from blood flow restoration after a period of oxygen deprivation, as seen in lung transplants or thoracoabdominal aortic surgery.

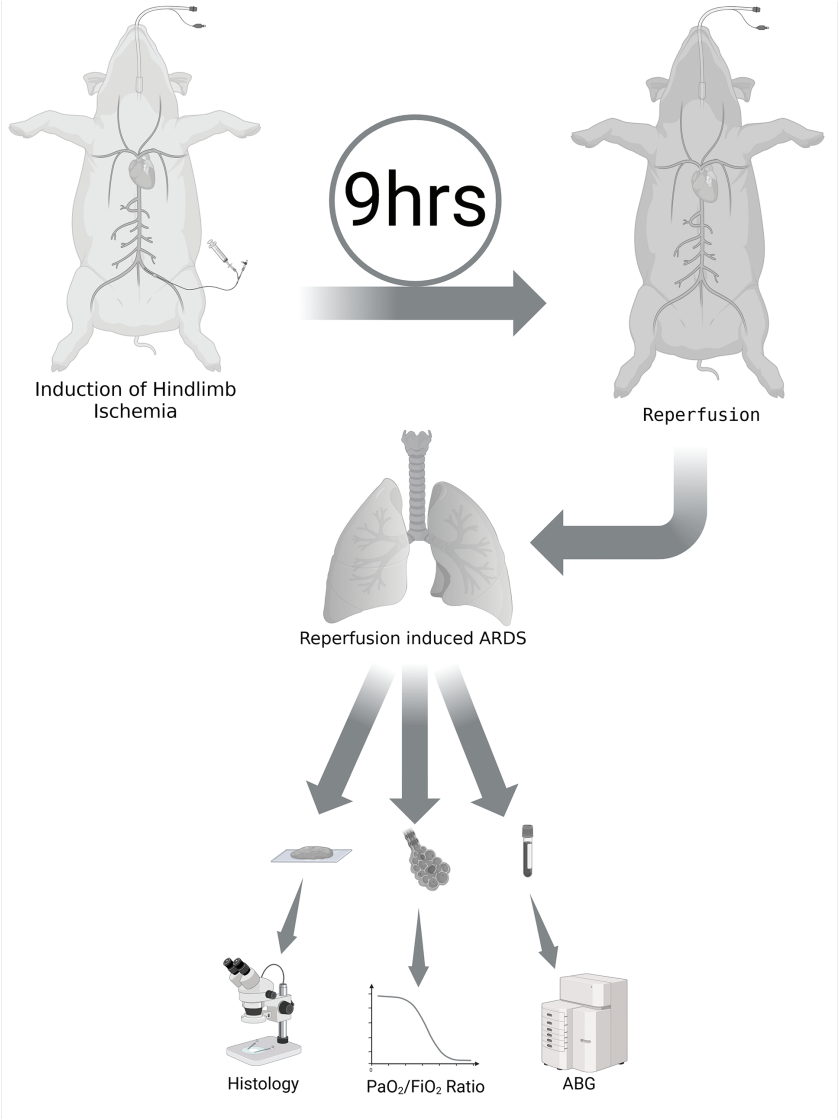

Figure 6 Experiment layout.

Pulmonary IRI involves clamping the pulmonary artery or the hilum of the lung for a defined period, followed by the restoration of blood flow. While this model helps examine injury mechanisms, it requires precise surgical skills and is time-consuming [6,18,19].

Our current approach, opting for an EIA and MSA occlusion IRI model over a pulmonary IRI model to induce ARDS, comes with unique advantages and disadvantages. Some of the former include the ability to investigate the systemic inflammatory cascade triggered by peripheral ischemia, mirroring human ARDS cases that occur with distal injuries. Because it mimics real-life pathophysiology, it might cause multi-system organ dysfunction from reperfusion injury in addition to ARDS, which contrasts with models that only target lung dysfunction [9]. Unlike pulmonary IRI, non-pulmonary IRI does not directly impair lung function, minimizing hypoxemia and hemodynamic instability within the lungs. This method offers a sterile approach, without the necessity of introducing systemic bacteria or DAMPs [15,20].

This model was designed with a focus on clinically relevant components, which is why the evaluation of biochemical markers was not included in the scope of this project. The animals presented symptoms typical of a lung injury, such as impaired gas exchange demonstrated by a dramatic decrease in the Horowitz index, but also confirmed with CT, ultrasound and histology. The sample size was limited to two animals, although the results remain promising. While combat-related trauma often involves polytrauma with extensive soft tissue and skeletal injuries, our model isolates IRI to establish a controlled platform for studying its direct role in ARDS pathogenesis. We do, however, acknowledge this limitation and see our model as complementary to more complex trauma models, providing foundational insights into isolated IRI contributions to ARDS. Further replication of this model in future experiments will help to validate the technique and enhance future experimental

use. Extending the duration of critical care periods will facilitate a more comprehensive progression of ARDS due to systemic reperfusion injury, providing greater insight into its pathophysiology and enhancing the model's relevance for future experimental applications.

Within the constraints of these limitations, this methodology for creating an ARDS model by inducing non-pulmonary IRI demonstrates promising results for further study. This model can be used in future studies to examine the pathophysiology and pathomechanism of ARDS.

Ethics Statement

(1) All the authors mentioned in the manuscript have agreed to authorship, read and approved the manuscript, and given consent for submission and subsequent publication of the manuscript.
(2) The authors declare that they have read and abided by the JEVTM statement of ethical standards including rules of informed consent and ethical committee approval as stated in the article.

Conflicts of Interest

The authors declare that they have no conflicts of interest.

Funding

This research has been funded by the Battlefield Shock and Organ Support Grant (ID: HU00011920072). This work was also supported by the German Research Foundation (DFG) under the Walter-Benjamin Program (grant number WI 6261/2-1).

Author Contributions

All authors have submitted substantially to the study, manuscript writing and editing.

Declaration of the Use of Generative AI and AI-Assisted Technologies in the Writing Process

During the preparation of this work the authors used (Chat GPT, Open AI, San Francisco, California) to improve readability and language. After using this tool, the authors reviewed and edited the content as needed and take full responsibility for the content of the publication.

REFERENCES

[1] Fard N, Saffari A, Emami G, Hofer S, Kauczor HU, Mehrabi A. Acute respiratory distress syndrome induction by pulmonary ischemia-reperfusion injury in large animal models. *J Surg Res*. 2014; 189(2): 274–84.
[2] Diamond M, Peniston HL, Sanghavi DK, Mahapatra S. Acute Respiratory Distress Syndrome. Treasure Island: StatPearls; 2025.
[3] Matute-Bello G, Frevert CW, Martin TR. Animal models of acute lung injury. *Am J Physiol Lung Cell Mol Physiol*. 2008; 295(3): L379–99.
[4] Obara H, Matsubara K, Kitagawa Y. Acute limb ischemia. *Ann Vasc Dis*. 2018; 11(4): 443–48.
[5] Lind B, Morcos O, Ferral H, et al. Endovascular strategies in the management of acute limb ischemia. *Vasc Specialist Int*. 2019; 35(1): 4–9.
[6] Fitridge R, Thompson M, editors. Mechanisms of Vascular Disease: A Reference Book for Vascular Specialists. Adelaide: University of Adelaide Press; 2011.
[7] Perkins ZB, Kersey AJ, White JM, et al. Impact of ischemia duration on lower limb salvage in combat casualties. *Ann Surg*. 2022; 276(3): 532–38.
[8] Pierro A, Eaton S. Intestinal ischemia reperfusion injury and multisystem organ failure. *Semin Pediatr Surg*. 2004; 13(1): 11–7.
[9] Wang HM, Bodenstein M, Markstaller K. Overview of the pathology of three widely used animal models of acute lung injury. *Eur Surg Res*. 2008; 40(4): 305–16.
[10] Meyerholz DK, Burrough ER, Kirchhof N, Anderson DJ, Helke KL. Swine models in translational research and medicine. *Vet Pathol*. 2024; 61(4): 512–23.
[11] Russ M, Kronfeldt S, Boemke W, Busch T, Francis RCE, Pickerodt PA. Lavage-induced surfactant depletion in pigs as a model of the Acute Respiratory Distress Syndrome (ARDS). *J Vis Exp*. 2016; (115): 53610.
[12] Goncalves-de-Albuquerque CF, Silva AR, Burth P, Castro-Faria MV, Castro-Faria-Neto HC. Acute respiratory distress syndrome: role of oleic acid-triggered lung injury and inflammation. *Mediators Inflamm*. 2015; 2015: 260465.
[13] Chen H, Bai C, Wang X. The value of the lipopolysaccharide-induced acute lung injury model in respiratory medicine. *Expert Rev Respir Med*. 2010; 4(6): 773–83.
[14] Tsikis ST, Fligor SC, Hirsch TI, et al. Lipopolysaccharide-induced murine lung injury results in long-term pulmonary changes and downregulation of angiogenic pathways. *Sci Rep*. 2022; 12(1): 10245.
[15] Sanchez PG, Pasrija C, Mulligan MJ, et al. A novel large animal model of acute respiratory distress syndrome induced by mitochondrial products. *Ann Surg*. 2017; 266(6): 1091–96.
[16] Rodriguez-Nuevo A, Zorzano A. The sensing of mitochondrial DAMPs by non-immune cells. *Cell Stress*. 2019; 3(6): 195–207.
[17] Abdullah S, Ghio M, Cotton-Betteridge A, et al. Succinate metabolism and membrane reorganization drives the endotheliopathy and coagulopathy of traumatic hemorrhage. *Sci Adv*. 2023; 9(24): eadf6600.
[18] Yabuki H, Watanabe T, Oishi H, Katahira M, Kanehira M, Okada Y. Muse cells and ischemia-reperfusion lung injury. *Adv Exp Med Biol*. 2018; 1103: 293–303.
[19] Weyker PD, Webb CA, Kiamanesh D, Flynn BC. Lung ischemia reperfusion injury: a bench-to-bedside review. *Semin Cardiothorac Vasc Anesth*. 2013; 17(1): 28–43.
[20] Nunns GR, Vigneshwar N, Kelher MR, et al. Succinate activation of SUCNR1 predisposes severely injured patients to neutrophil-mediated ARDS. *Ann Surg*. 2022; 276(6): e944–e54.